Revision Date: 23 March 2010 [fludioxonil_04]

Title: Turgor and net ion flux responses to activation of the osmotic MAP kinase cascade by fludioxonil in the filamentous fungus *Neurospora crassa*.

Running Title: Hyperosmotic-induced transient responses in *Neurospora*

Subject Category: Physiology

Roger R. Lew*
Department of Biology, York University, Toronto, Ontario Canada,
*Corresponding author. Mailing address: Department of Biology, York University, 4700 Keele Street, Toronto, Ontario M3J 1P3, Canada. Phone: 416–736–5243. Fax: 416–736–5698. E–mail: planters@yorku.ca.

Preprint published in Fungal Genetics and Biology, **8**(47), p. 721-726
DOI: 10.1016/j.fgb.2010.05.007

SUMMARY

The internal hydrostatic pressure (turgor) of the filamentous fungi *Neurospora crassa* is regulated at about 400–500 kiloPascals, primarily by an osmotic MAP kinase cascade which activates ion uptake from the extracellular medium and glycerol synthesis. The phenylpyrrole fungicide fludioxonil activates the osmotic MAP kinase cascade, resulting in cell death. Turgor, the electrical potential and net ion fluxes were measured after treatment with fludioxonil. In wildtype, fludioxonil causes a hyperpolarization of the plasma membrane and net H^+ efflux from the cell, consistent with activation of the H^+-ATPase. At the same time, net K^+ uptake occurs, and turgor increases (about 2-fold). None of these changes are observed in the *os–2* mutant (which lacks a functional MAP kinase, the last of the three kinases in the osmotic MAP kinase cascade). Tip growth ceases as hyperpolarization, net ion flux changes, and turgor increases begin. The results corroborate a multi-pathway response to hyperosmotic stress that includes activation of plasma membrane transport. The relation to cell expansion (tip growth) is not direct. Increases in turgor due to ion transport might be expected to increase growth rate, but this does not occur. Instead, there must be a complex interplay of regulation between growth and the turgor driving force.

INTRODUCTION

Fungi often maintain a high internal hydrostatic pressure (turgor) during cellular expansion (Lew et al., 2004), a trait also common in cells of higher plants and algae (Zimmerman, 1978). In *Neurospora crassa*, when subjected to hyperosmotic stress, fungal turgor decreases, but then recovers rapidly, within an hour (Lew and Nasserifar, 2009). Turgor recovery is caused by two different mechanisms: *de novo* synthesis of osmolytes (Ellis et al., 1991) and ion accumulation from the extracellular medium (Lew et al., 2006). Both responses are activated by an osmotic MAP kinase cascade (O'Rourke et al., 2002; Krantz et al., 2006). A histidine kinase sensor, OS–1 (Alex et al., 1996; Miller et al., 2002), activates the kinase cascade MAPKKK OS–4 and MAPKK OS–5 (Fujimura et al., 2003), and MAPK OS–2 (Zhang et al., 2002). Upon activation of OS–2, one response is the expression of a number of genes, including genes for glycerol synthesis (Noguchi et al., 2007) as well as sugar and amino acid metabolism (Irmler et al., 2006); at least one of the transcription factors activated by OS–2 has been identified, ATF–1 (Yamashita et al., 2008). Independent of gene expression, the plasma membrane H^+-ATPase and ion uptake are rapidly (within 10-15 min) activated by hyperosmotic treatment (Lew et al., 2006) and can regulate turgor in the absence of glycerol synthesis (in the osmosensitive *cut* mutant) (Lew and Levina, 2007).

A useful tool in analysis of the osmotic response is the phenylpyrrole fungicide fludioxonil (Pillonel and Meyer, 1997). It activates the osmotic MAP kinase cascade directly (Zhang et al., 2002; Irmler et al., 2006). Mutants in the sensor and kinase cascade (*os–1*, *os–4*, *os–5*, *os–2*) are insensitive to the fungicide (Fujimura et al., 2000; Ochiai et al., 2001; Zhang et al., 2002). Fludioxonil activation of the osmotic MAP kinase cascade occurs at the OS–1 osmosensor; *os–1* mutant alleles fall into two classes of resistance (high and low) that are related to the site of the mutation in the OS–1 gene (Ochiai et al., 2001). When an OS–1 homolog (*HIK1* from the rice blast fungus *Pyricularia oryzaefrom*) is expressed in *Saccharomyces cerevisiae* (which lacks a homolog of *OS–1* and is normally insensitive to the fludioxonil), it confers sensitivity to fludioxonil (Motoyama et al., 2005). Another yeast (*Candida albicans*) contains a homolog of the *OS–1* gene and is sensitive to fludioxonil (Ochiai et al., 2001). Thus, the phenylpyrrole fungicide is specific to the osmotic MAP kinase cascade, and offers an

alternative way to activate the osmotic MAP kinase cascade and explore its mechanism in detail, without perturbing the cells with the stress of high osmolarity. We have previously shown that fludioxonil causes hyperpolarization of the plasma membrane potential in wildtype, a response that is absent in the *os–2* mutant (Lew and Levina, 2007). In this paper, the effect of fludioxonil on turgor, potential, and ion fluxes is demonstrated directly in wildtype and, as a control, the fludioxonil-insensitive *os–2* mutant. The results corroborate previous work with osmotic responses: that the osmotic MAP kinase cascade activates ion transport to recover turgor.

METHODS

Strains. Stock cultures of wildtype (FGSC 2489) and *os-2* (allele UCLA80, FGSC No. 2238) were obtained from the Fungal Genetics Stock Center (School of Biological Sciences, University of Missouri, Kansas City, Missouri, USA)(McCluskey, 2003). Stock cultures of the strains were maintained on Vogel's (plus 1.5% (w/v) sucrose and 2.0% (w/v) agar) medium (VM) (Vogel, 1956).

Culture Preparation for Experiments. Cultures were prepared by inoculating conidia onto strips (2.5 X 6 cm) of dialysis tubing that overlay the VM in Petri dishes and incubated at 28 ºC overnight. The dialysis tubing was cut with a razor blade to a size of about 1 X 3 cm, which included the growing edge of the colony, placed inside the cover of a 30 mm Petri dish, and immobilized on the bottom with narrow strips of masking tape. The culture was flooded with 3 ml of a modified buffer solution (BS) (in mM): $CaCl_2$ (0.05), $MgCl_2$ (0.05), and sucrose (150), unbuffered. The use of unbuffered media with low salt concentrations was to avoid 'hidden' H^+ fluxes due to H^+ binding to buffer (Arif et al., 1995; Messerli et al., 2006) and avoid high background concentrations of K^+, which would decrease the signal to noise ratio of K^+ flux measurements. Since the fungal colonies were grown on nutrient-replete Vogel's medium, there was carry over of K^+. Background [K^+] in the submersed fungal colonies was about 230 ± 106 μM (n=24). The pH remained fairly constant (5.81 ± 0.37, n=27) over the course of the experiments. Growth of hyphae at the colony edge resumed within 15 min after flooding with the modified BS.

Electrical Measurements. Large trunk hyphae (10–20 μm diameter) about 0.5 cm behind the colony edge were selected for potential and concomitant net ion flux measurements. The hypha was first impaled with a micropipette, then the ion-selective probe was positioned nearby for measurements of the ion flux.

Ion-flux Measurements. Measurements with the ion-selective probe has been described in detail previously (Lew, 1999; Lew et al., 2006; Lew and Levina, 2007). The following ion-selective cocktails were used (Sigma–Aldrich): H^+ (hydrogen ionophore II-cocktail A, catalogue no. 95297); K^+ (potassium ionophore I-cocktail A, catalogue no. 60398 [modified by replacing 25% w/w 1,2-dimethyl-3-nitrobenzene with 25% w/w 2-nitrophenyl octyl ether (Messerli et al., 2006)]). The ion-selective probes were calibrated at pH 7, 6, 5 and 4 (H^+) using pH standards (Fisher) or 0.01, 0.1, 1.0, 10.0 mM KCl (K^+). The concentration of the selected ion was measured at two positions: as near to the hyphal wall as possible, and 20 μm away, at a frequency of about 0.3 Hz. The differences in ion concentrations at the hypha and 20 μm from the hypha were converted to net ion flux (J, nmol m^{-2} s^{-1}) with the following equation, which accounts for the cylindrical geometry of the hyphae:

$$J = \frac{D}{r}\frac{(c_2 - c_1)}{\ln\left(\frac{r_2}{r_1}\right)}$$

where D is the diffusion coefficient (H^+, $9.31 \cdot 10^{-9}$ m^2 s^{-1}; K^+, $1.96 \cdot 10^{-9}$ m^2 s^{-1}); r is the hyphal radius; c_1 and c_2 the concentrations at the two excursion points; and r_1 and r_2 the distances from the hyphal centre to the two excursion points (Henriksen et al., 1992). Background measurements were performed 100 μm above the hypha twice during the experiments (during the pre-treatment measurement and at the end of the experiment); these were used to correct any offset in the measured net ion flux.

Net influxes are shown as negative fluxes; net effluxes are shown as positive fluxes.

After about 18 min of recording the electrical potential and the net ion flux, the hyphae were treated with fludioxonil, added as an 0.5 ml aliquot of 0.8 mM fludioxonil in modified BS, and measurements continued for about 14 min.

Turgor Measurements. Impalements were made on large trunk hyphae of cultures prepared the same way as for electrophysiological and ion flux measurements. The technique has been described in detail previously (Lew et al., 2004, 2006; Lew and Levina, 2007). Large-aperture micropipettes were fabricated using a double-pull technique. The micropipette was filled with low-viscosity silicone oil (polydimethylsiloxane, 1.5×10^{-6} m^2 s^{-1}; Dow Corning), and mounted in a holder attached to a micrometer-driven piston by thick-wall teflon tubing. Pressure was measured with a transducer (XT-190-300G; Kulite Semiconductor Products) mounted on the holder. After impalement, the internal hydrostatic pressure pushed the meniscus between the silicone oil and cell sap into the micropipette; the pressure required to bring the meniscus back to the tip was a measure of the turgor. After turgor measurements for ~6 min, 0.5 ml of 0.8 mM fludioxonil in modified BS was added to the dish and turgor measurements continued for about 40 min. If the micropipette tip became plugged during the turgor measurements, every attempt was made to re-impale the same hypha, or another one nearby, with a fresh micropipette.

Statistical analysis. Data are shown as mean ± SD (sample size) unless stated otherwise. Independent two-tail t-tests and non-linear regressions were performed in Excel (Microsoft), SYSTAT (Systat, Inc.), or KaleidaGraph (Synergy Software).

RESULTS

Fludioxonil affects both turgor and tip growth of wildtype. In the modified (low salt, no buffer) solution, the initial turgor of the *os–2* mutant (512 ± 42 kiloPascal, n=11) was significantly lower than wildtype turgor (627 ± 29 kiloPascal, n=11) ($P<10^{-8}$) (Fig. 1), confirming previous turgor comparisons (Lew et al., 2006) in 'normal' buffered solution containing sucrose (133 mM), Mes (10 mM, pH 5.8 with KOH), KCl (10 mM) and $CaCl_2$ and $MgCl_2$ (both 1 mM). Within 12 minutes of fludioxonil treatment, wildtype turgor began to increase, reaching about 1100 kiloPascal after 36 minutes. Turgor of the fungicide-insensitive *os–2* mutant was unaffected by fludioxonil treatment. Under the same conditions, tip growth rates of wildtype declined to zero within about 12 minutes, while *os–2* growth rates were unaffected (Fig. 1).

Fludioxonil hyperpolarizes the potential in wildtype. Treatment with fludioxonil caused a hyperpolarization in wildtype, but not the *os2* mutant (Fig. 2). The initial potentials of the two strains were similar (wildtype, –150 ± 25 mV, n=16; *os–2* mutant, –144 ± 24 mV, n=16; P=0.50). Fludioxonil caused a hyperpolarization of the wildtype potential to –170 ± 28 (n=13) while the potential of the *os–2* mutant was unaffected (–140 ± 29 mV, n=13). The *change* in potential caused by fludioxonil in wildtype (–18 ± 9 mV, n=13) was significantly more negative than the *os–2* mutant (+6 ±12 mV, n=13) ($P<10^{-3}$) (Fig. 2). These electrical responses —wildtype hyperpolarization and no response for the *os–2* mutant— are similar to the responses to hyperosmotic stress (Lew et al., 2006).

Fludioxonil activates net H^+ efflux in wildtype. A likely cause of the hyperpolarization in wildtype is activation of the plasma membrane H^+-ATPase. This is corroborated by fludioxonil-induced shift to net H^+ efflux in wildtype (Fig. 3). The figure shows examples of individual experiments, and compiled electrical and net flux changes for net H^+ flux measurements. Hyperpolarization (by –15.2 ± 4.2 mV, n = 6) and a shift to net H^+ efflux a change of +7.8 ± 4.4 nmole m^{-2} s^{-1}, n = 6) was observed in wildtype, but neither was observed in the *os–2* mutant, for which the potential changed +3.2 ± 13.2 mV (n = 6) and net H^+ flux shifted to inward (–14.9 ± 25.3 nmole m^{-2} s^{-1}, n = 6). The differences in electrical response and H^+ flux responses were statistically significant (P = 0.004 and P = 0.028, respectively).

Fludioxonil activates net K^+ uptake in wildtype. Much of turgor recovery can be attributed to ion uptake (in addition to glycerol synthesis). The hyperpolarization caused by fludioxonil in wildtype (–19.9 ± 11.0 mV, n = 7) is accompanied by a shift to net K^+ uptake (–40.1 ± 46.7 nmole m^{-2} s^{-1}, n = 5) (Fig. 4). Neither of these responses were observed in the fludioxonil-insensitive *os–2* mutant: the potential changed by +9.3 ± 11.7 mV (n = 7) and net K+ flux shifted to outward by +11.0 ± 25.6 nmole m^{-2} s^{-1} (n = 6). The differences were statistically significant (P = 0.0002 and P = 0.023, respectively).

DISCUSSION

Walled cells of fungi, plants and algae normally accumulate osmolytes to levels higher than concentrations in the extracellular milieu, thereby generating an internal hydrostatic pressure (turgor). Turgor is believed to drive cellular expansion, and, in filamentous fungi, intrahyphal pressure gradients may move cytoplasm forward with the growing tip (Lew, 2005; Ramos-García et al., 2009). Not all hyphal organisms regulate turgor (Kaminskyj et al., 1992; Lew et al., 2004). Ameboidal fungal cells (the *slime* mutant of *N. crassa*) and oomycetes (Money & Harold, 1993) can grow in the absence of turgor. So, alternative mechanisms of growth occur, but even so, the existence of a causal relation between turgor and cell expansion is widely accepted (Bartnicki-García et al., 2000).

Hyperosmotic stress has rapid effects on the filamentous fungi *Neurospora crassa*: Turgor drops immediately, hyphal volumes shrink, and growth stops (Lew and Nasserifar, 2009). All of these responses occur within a minute or so of hyperosmotic treatment. Turgor and growth recovery commence within 10–20 min. Recovery occurs concomitantly with hyperpolarization of the plasma membrane potential. The hyperpolarization is presumably due to activation of the plasma membrane H^+-ATPase (since net H^+ efflux commences with a similar time course). It does not require *de novo* protein synthesis (Lew et al., 2006). Thus the osmoresponse machinery is already in place without recourse to gene expression. Net K^+ uptake is presumably responsible for much of the turgor

recovery (in addition to glycerol synthesis, Lew and Levina, 2007), which is complete within about 60 minutes of the onset of hyperosmotic stress.

There are indications that multiple pathways contribute to turgor regulation. Many *os* mutants of the osmotic MAP kinase cascade still retain the ability to synthesize glycerol in response to hyperosmotic stress. Some glycerol accumulation (Ellis et al., 1991) and lower activation of ion uptake (Lew et al., 2006), as well as phosphorylation of the *OS–2* MAP kinase (Noguchi et al., 2007) are observed in mutants of the *os–1* osmosensor. Glycerol synthesis in response to hyperosmotic stress is also observed in mutants of other components of the osmotic MAP kinase cascade (*os–2*, *os–4*, *os–5*) (Fujimura et al, 2000), and *os–2* mutants still retain some ability to regulate turgor (Lew et al., 2006). The nature of the alternative pathways is as yet incompletely understood. The magnitude of the osmotic stress affects the osmoresponse. Higher osmotic stress induces a rapid transient depolarization of the plasma membrane potential that is not observed at lower osmotic stress (Lew and Nasserifar, 2009). Even in the absence of a functional osmosensor (*os–1*), higher osmotic stress causes phosphorylation of the *OS–2* MAP kinase (Noguchi et al., 2007). A kinase activator (*PTK2*) of the plasma membrane H^+-ATPase contributes to turgor regulation in a pathway separate from the osmotic MAP kinase cascade (Lew and Kapishon, 2009). These results support the presence of different pathways, with differential sensitivity to osmotic stress. Notably, the activation of the MAP kinase cascade by fluxioxonil 'mimics' the effects of low osmotic stress (Noguchi et al., 2007), and therefore it may selectively activate the MAP kinase cascade in *N. crassa*. Thus, fludioxonil should make it possible to explore specifically the effects of an activated MAP kinase cascade separate from other osmoresponse pathways, and for this reason was used for direct measurements of growth, turgor, potential changes and ion fluxes.

When subjected to treatment with fludioxonil, fungal hyphae respond within about 10 minutes, consistent with activation of the osmotic MAP kinase cascade. In wildtype, the hyperpolarization of the potential and activation of net H^+ efflux and net K^+ influx are all quite similar to the responses after hyperosmotic treatment. Unlike the turgor recovery observed after hyperosmotic treatment, fludioxonil induces a very significant increase in hyphal turgor, almost doubling from its normal value of about 630 to about 1100 kiloPascal. The increased turgor is the likely cause of the eventual hyphal bursting reported in wildtype, but not the *os–2* mutant (Zhang et al., 2002). The *os–2* mutant is an effective control for osmotic MAP kinase cascade mediated effects. In the *os–2* mutant, after fludioxonil treatment, the absence of a hyperpolarization and unaffected growth confirms previous results (Lew and Levina, 2007), net ion fluxes are unaffected (K^+), or trend to higher net influx in the case of H^+, and turgor is unaffected.

Wildtype hyphal tip growth stops at about the same time that turgor begins to increase. During turgor recovery after osmotic stress, there appears to be a reasonable correlation between rates of tip growth and turgor (Lew and Nasserifar, 2009). One might expect that tip growth rates would accelerate as turgor increased after fludioxonil treatment, but this is not the case. Other mechanisms, as yet unknown, regulate the process of tip growth separately from turgor during activation of the osmotic MAP kinase cascade.

In summary, activation of the MAP kinase cascade by fludioxonil in the absence of hyperosmotic stress causes a specific set of electrical responses: activation of the H^+-ATPase and net K^+ uptake. These responses are probably sufficient to cause a dramatic increase in turgor, since glycerol synthesis occurs later than the electrical responses in response to osmotic stress (Lew and Levina, 2007; Shanar and Nasserifar, 2009). The arrest of tip growth prior to elevation of turgor suggests a complex interplay of physiological poise and growth during activation of the cascade.

ACKNOWLEDGEMENTS

This research was supported in part by a discovery grant from the Natural Sciences and Engineering Research Council of Canada (R.R.L.). Ion-flux measurements were performed at the BioCurrents Research Center, Marine Biological Laboratory, Woods Hole, MA; R. R. L. is grateful for the hospitality of the Director, Peter J. S. Smith, and his colleagues.

REFERENCES

Alex, L. A., Borkovich, K. A. & Simon, M. I. (1996). Hyphal development in *Neurospora crassa*: involvement of a two-component histidine kinase. *Proc Natl Acad Sci USA* **93,** 3416–3421.

Arif I, Newman IA, Keenlyside N. (1995). Proton flux measurements from tissues in buffered solutions. *Plant, Cell and Environment* **18,** 1319–1324.

Bartnicki-Garcia, S., Bracker, C. E., Gierz, G., Lopez-Franco, R. & Lu, H. (2000). Mapping the growth of fungal hyphae: Orthogonal cell wall expansion during tip growth and the role of turgor. *Biophys J* **79,** 2382–2390.

Ellis, S. W., Grindle, M. & Lewis, D. H. (1991). Effect of osmotic stress on yield and polyol content of dicarboximide-sensitive and –resistant strains of *Neurospora crassa*. *Mycol Res* **95,** 457–464.

Fujimura, M., Ochiai, N., Ichiishi, A., Usami, R., Horikoshi, K. & Yamaguchi, I. (2000). Sensitivity to phenylpyrrole fungicides and abnormal glycerol accumulation in *os* and *cut* mutant strains of *Neurospora crassa, J. Pesticide Sci*. **25,** 31–36.

Fujimura, M., Ochiai, N., Oshima, M., Motoyama, T., Ichiishi, A., Usami, R., Horikoshi, K. & Yamaguchi, I. (2003). Putative homologs of *SSK22* MAPKK kinase and *PBS2* MAPK kinase of *Saccharomyces cerevisiae* encoded by *os–4* and *os–5* genes for osmotic sensitivity and fungicide resistance in *Neurospora crassa*. *Biosci Biotechnol Biochem* **67,** 186–191.

Henriksen, G.H., Ramam, D.R., Walker, L.P. & Spanswick, R.M. (1992). Measurement of net fluxes of ammonium and nitrate at the surface of barley roots using ion-selective microelectrodes. *Plant Physiology* **99,** 734–747.

Irmler, S., Rogniaux, H., Hess, D. & Pillonel, C. (2006). Induction of OS–2 phosphorylation in *Neurospora crassa* by treatment with phenylpyrrole fungicides and osmotic stress. *Pesticide Biochemistry and Physiology* **84,** 25–37.

Kaminskyj, S. G. W., Garrill, A. & Heath, I. B. (1992). The relation between turgor and tip growth in *Saprolegnia ferax*: turgor is necessary, but not sufficient to explain apical extension rates. *Exp Mycol* **16,** 64–75.

Krantz, M., E. Becit, E. & Hoffmann, S. (2006). Comparative genomics of the HOG-signaling system in fungi. *Curr Genet* **49,** 137–151.

Lew, R. R. (1999). Comparative analysis of Ca^{2+} and H^{+} flux magnitude and location along growing hyphae of *Saprolegnia ferax* and *Neurospora crassa*. *European Journal of Cell Biology*. **78,** 892–902.

Lew, R. R. (2005). Mass flow and pressure-driven hyphal extension in *Neurospora crassa*. *Microbiology (SGM)* **151,** 2685–2692.

Lew, R. R. (2007). Ionic currents and ion fluxes in *Neurospora crassa* hyphae. *J Exp Bot* **58,** 3475–3481.

Lew, R. R. & Levina, N. N. (2007). Turgor regulation in the osmosensitive cut mutant of *Neurospora crassa*. *Microbiology*. **153,** 1530–1537.

Lew, R. R. & Nasserifar, S. (2009). Transient responses during hyperosmotic shock in the filamentous fungus *Neurospora crassa*. *Microbiology*. **155,** 903–911.

Lew, R. R., Levina, N. N., Walker, S. K. & Garrill, A. (2004). Turgor regulation of hyphal organisms. *Fungal Genet Biol* **41,** 1007–1015.

Lew, R. R., Levina, N. N., Shabala, L., Anderca, M. I. & Shabala, S. N. (2006). Role of a mitogen-activated protein kinase cascade in ion flux-mediated turgor regulation in fungi. *Eukary Cell* **5,** 480–487.

McCluskey, K. (2003). The Fungal Genetics Stock Center: from molds to molecules. *Adv Appl Microbiol* **52,** 245–262.

Messerli M. A., Robinson K. R. & Smith P. J. S. (2006). Electrochemical sensor applications to the study of molecular physiology and analyte flux in plants. *In* Volkov, A. G. (ed.) Plant Electrophysiology – Theory and Methods. Springer. pp. 73–107.

Miller, T. K., Renault, S. & Selitrennikoff, C. P. (2002). Molecular dissection of alleles of the osmotic–1 locus of *Neurospora crassa*. *Fungal Genet Biol* **35,** 147–155.

Money, N. P. & Harold, F. M. (1993). Two water molds can grow without measurable turgor pressure. *Planta* **190,** 426–430.

Motoyama, T., Ohira, T., Kadokura, K., Ichiishi, A., Fujimura, M., Yamaguchi, I. & Kudo, T. (2005). An Os–1 family histidine kinase from a filmentous fungus confers fungicide-sensitivity to yeast. *Current Genetics* **47,** 298–306.

Noguchi, R., Banno, S., Ichikawa, R., Fukumori, F., Ichiishi, A., Kimura, M., Yamaguchi, I. & Fujimura, M. (2007). Identification of OS–2 MAP kinase-dependent genes induced in response to osmotic stress, antifungal agent fludioxinil, and heat shock in *Neurospora crassa*. *Fungal Genet Biol* **44,** 208–218.

O'Rourke, S. M., Herskowitz, I. & O'Shea, E. K. (2002). Yeast go the whole HOG for the hyperosmotic response. *Trends Genet* **18,** 405–412.

Ochiai, N., Fujimura, M., Motoyama, T., Ichiishi, A., Usami, R., Horikoshi, K. & Yamaguchi, I. (2001). Characterization of mutations in the two-component histidine kinase gene that confer fludioxonil resistance and osmotic sensitivity in the *os–1* mutants of *Neurospora crassa*. *Pest Management Science* **57,** 437–442.

Pillonel, C. & Meyer, T. (1997). Effect of phenylpyrroles on glycerol accumulation and protein kinase activity of *Neurospora crassa*. *Pestic. Sci*. **49,** 229–236.

Ramos-García, S.L., Roberson, R.W., Freitag, M., Bartnicki-García, S. & Mouriño-Pérez, R.R. (2009). Cytoplasmic bulk flow propels nuclei in mature hyphae of *Neurospora crassa*. *Eukaryotic Cell*. **8,** 1880–1890.

Vogel, H. J. (1956). A convenient growth medium for *Neurospora*. *Microbial Genetics Bulletin* **13,** 42–46.

Yamashita, K., Shiozawa, A., Watanabe, S., Fukumori, F., Kimura, M. & Fujimura, M (2008). ATF–1 transcription factor regulates the expression of *ccg–1* and *cat–1* genes in response to fludioxonil under OS–2 MAP kinase in *Neurospora crassa*. *Fungal Genetics and Biology* **45,** 1562–1569.

Zhang Y., Lamm, R., Pillonel, C., Lam, S. & Xu, J-R. (2002). Osmoregulation and fungicide resistance: The *Neurospora crassa os–2* gene encodes a *HOG1* mitogen-activated protein kinase homologue. *Appl Environ Microbiol* **68,** 532–538.

Zimmerman, U. (1978). Physics of turgor- and osmoregulation. *Annual Review of Plant Physiology* **29,** 121–148.

FIGURES

Fig. 1. Turgor and growth responses to fludioxonil. The initial turgor (A), turgor response (B) and growth responses (C) are shown for wildtype (circles) and the *os–2* mutant (triangles). Individual data and means ± SD are shown for initial turgor measurements. For turgor responses, individual experiments (lines) and means are shown. For growth rates, the means ± SE are shown (n = 28 for wildtype, 46 for the *os–2* mutant).

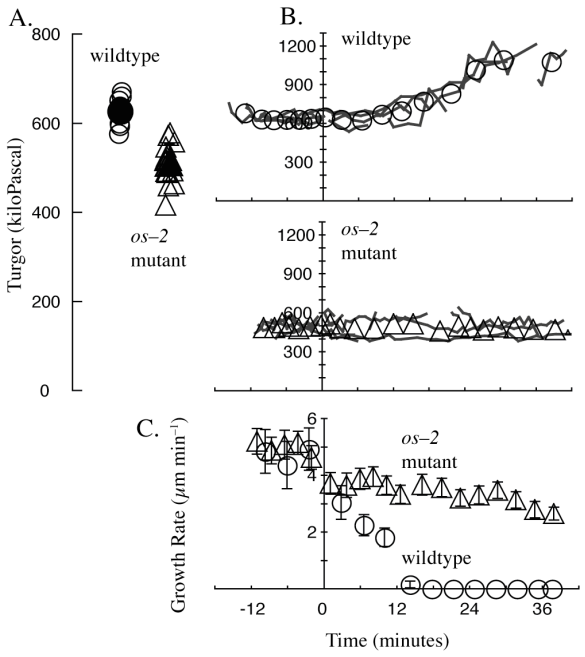

Fig. 2. Electrical responses to fludioxonil. Potential measurements are compiled from all experiments. The initial electrical potential (circles), final potential after fludioxonil treatment (squares) (A, left panel) and change in potential caused by fludioxonil (triangles) (B, right panel) are shown for wildtype and the *os–2* mutant as shown. The results of two-tail t-tests are indicated in the graph.

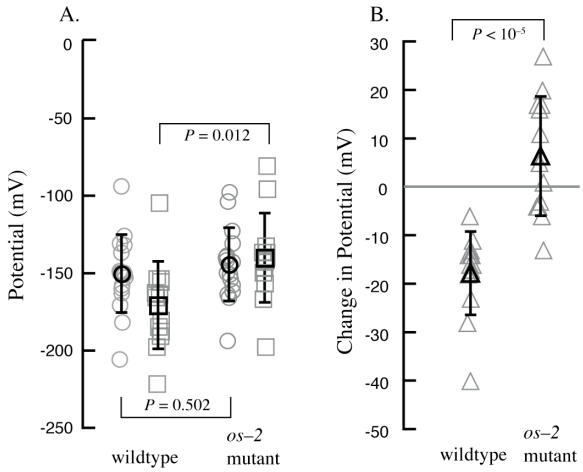

Fig. 3. Examples of membrane potential and net H^+ flux responses to fludioxonil treatment for wildtype (A, upper left panel) and the *os–2* mutant (B, lower left panel). Summary data for the *changes* in potential and net H^+ fluxes are shown in the right panels (C).

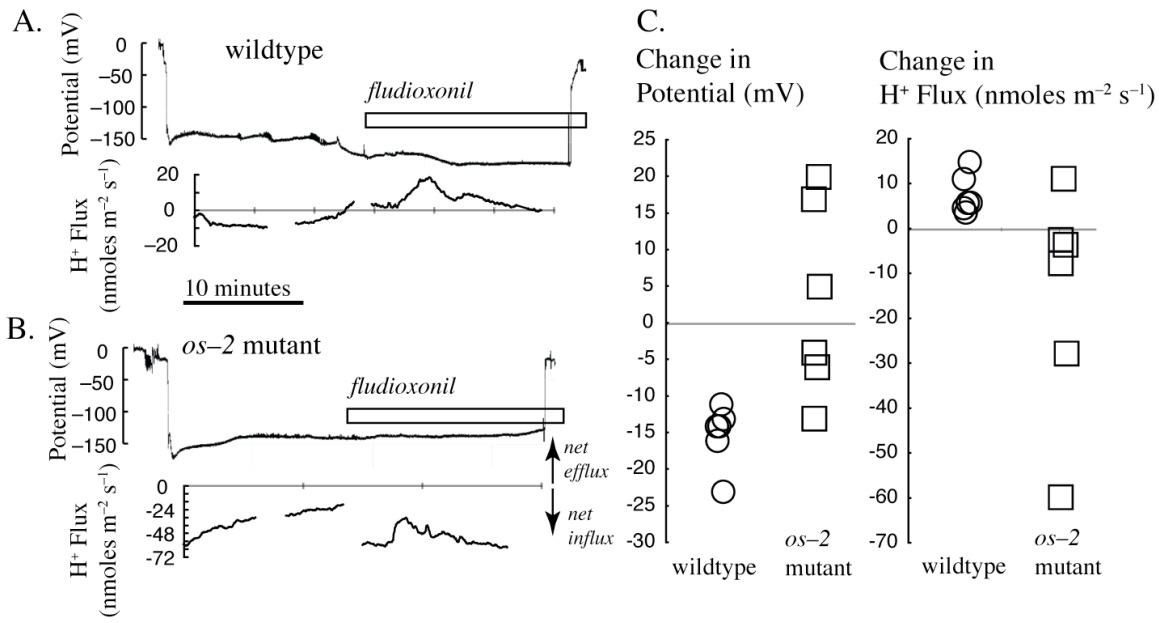

Fig. 4. Examples of membrane potential and net K^+ flux responses to fludioxonil treatment for wildtype (A, upper left panel) and the *os–2* mutant (B, lower left panel). Summary data for the *changes* in potential and net K^+ fluxes are shown in the right panels (C).